

Research on the interface characteristics of coal gangue with different geosynthetic reinforcements

Xudong Zhao^{1,2} , Pengfei Gao³, Weichao Liu^{1,2}, Yan Yang⁴, Lingxiao Meng^{5,6}, Guangqing Yang^{1,2}, Yingdong Xu^{5,6}

¹Ministry of Education, Shijiazhuang Tiedao University, Key Laboratory of Roads and Railway Engineering Safety Control, 050043, Shijiazhuang, China.

²Shijiazhuang Tiedao University, School of Civil Engineering, 050043, Shijiazhuang, China.

³Qingdao Hailutong Engineering Quality Inspection Co., Ltd., 266200, Qingdao, China.

⁴Shijiazhuang Tiedao University, School of Traffic and Transportation, 050043, Shijiazhuang, China.

⁵China Construction Infrastructure Corporation Limited, 100000, Beijing, China.

⁶China State Construction Engineering Corporation Limited, 100029, Beijing, China.

e-mail: liuweichao@stdu.edu.cn, 419784952@qq.com, gaopf96@163.com, tashiyangyan@sina.com, muluo690119@163.com, gtsyang@163.com, jiaqianliu@163.com

ABSTRACT

Coal gangue occupies substantial land resources. Using coal gangue as reinforcement fill material is an effective utilization method. The characteristics of the soil-reinforcement interface influence the safety and stability. Large-scale direct shear tests were conducted to study the interface characteristics of coal gangue with polypropylene woven geotextile, welded steel-plastic geogrid, and high-density polyethylene uniaxial geogrid. The tests revealed that the shear stress-shear displacement relationship is nonlinear and positively correlated with normal stress, with the breakage of burnt coal gangue particles observed during the process. The maximum shear stress and shear strength index of the interface for the three geosynthetics reinforced coal gangue are in the order of uniaxial high-density polyethylene (HDPE) geogrid showing the highest reinforcement strength, followed by the welded steel-plastic geogrid, with the polypropylene woven geotextile having the lowest strength. After HDPE geogrid reinforcement, interface friction angle slightly changes, but cohesion significantly increases, with an increase of 1156.9%. Considering the interface interactions, among the three geosynthetic materials, HDPE geogrid exhibits the most effective reinforcement effect on coal gangue, followed by the welded steel-plastic geogrid. The geotextile shows the least effectiveness in reinforcing burnt coal gangue. For reinforced coal gangue projects, HDPE geogrid is recommended as the reinforcing material.

Keywords: geotextile; geogrids; reinforced soil; interface friction characteristics; direct shear test.

1. INTRODUCTION

When openly stockpiled, coal gangue, the solid waste from coal mining and washing, not only occupies significant land area but also pollutes air, soil, and water resources, posing risks such as landslides and severely impacting local ecology and resident safety. Therefore, controlling and utilizing coal gangue is crucial. In engineering, coal gangue is utilized for constructing roadbeds [1] and as filler in reinforced earth retaining walls [2], thereby reducing the volume of gangue and soil excavation and yielding substantial economic benefits. Reinforced earth slopes and reinforced earth retaining walls are prevalent reinforcement structures. They offer numerous benefits, including construction convenience, minimal land occupation, low cost, reduced environmental impact, excellent seismic resistance, and strong adaptability. When coal gangue is used as filler in reinforced structures, the interface characteristics between the gangue and reinforcement materials are vital for the stability and deformation of the overall structure.

Global scholars have conducted studies on the interface properties of reinforced soil. WU *et al.* [3] used direct shear tests to examine the interface characteristics between fly ash, plastic tensile geogrids, and geonets, finding that the direct shear coefficient is usually less than 1, suggesting a range of 0.7 to 0.8. HUANG and LIU [4] and PENG and LIU [5] observed higher interface strength in direct shear tests than in pull-out tests. YANG *et al.* [6] conducted direct shear tests to investigate the residual strength characteristics of gabion networks

combined with coal gangue of varying soil content. The results indicate that the residual strength increases with an increase in normal load and that the residual strength is not significantly different from the peak strength. XIAO *et al.* [7] discovered that the shear stress at the interface between triaxial geogrids and sandy soil gradually decreases with increased shear rate. Furthermore, under the same normal load conditions, the peak shear stress between triaxial geogrids and sandy soil is consistently higher than that of uniaxial and biaxial geogrids. PENG *et al.* [8] investigated the interface characteristics between gabion networks and coal gangue through direct shear tests. The results indicate that the gabion networks and coal gangue exhibit favorable interfacial friction characteristics, with a direct shear interfacial friction coefficient greater than 1. ZHOU *et al.* [9] conducted large-scale direct shear tests to investigate the interface characteristics between construction waste and various geosynthetics, including biaxial plastic geogrids, biaxial fiberglass geogrids, and nonwoven geotextiles. The interface between construction waste and biaxial plastic geogrid exhibits the highest peak shear stress at consistent moisture content. In contrast, the interfaces between construction waste, biaxial fiberglass geogrids, and nonwoven geotextiles demonstrated similar peak shear stresses. WANG *et al.* [10] carried out a comprehensive study using large-scale direct shear tests to assess the impact of various geogrid types on the interfacial behavior with gravel. The research established that the interfacial shear strength of gravel, when combined with four different geogrids, increases in the sequence of triaxial geogrid, biaxial geogrid, short-rib uniaxial geogrid, and long-rib uniaxial geogrid. MARKOU [11] utilized direct shear tests to discern geotextile surface characteristics, such as pore size, influence the interface properties between sandy soil and the geotextile fabric. VIEIRA *et al.* [12] conducted direct shear and pull-out tests to investigate the interface performance between fines in construction waste and three types of geosynthetic materials. The study by LIU *et al.* [13] delineated a correlation between the augmented tensile strength of geogrids and an increase in the interfacial shear strength with soil. This enhancement is attributed to three pivotal factors: the frictional resistance at the interface of soil and geogrid ribs, the intrinsic shear strength of soil confined by the geogrid apertures, and the additional support provided by the geogrid's transverse ribs. WANG *et al.* [14] conducted large-scale direct shear tests to analyze the impact of compaction and normal stress on the shear characteristics of the interface. The results indicated that the interface's peak shear stress increased with compaction and normal stress. In contrast, the apparent cohesion of the interface rose with compaction, and the apparent friction angle showed the opposite trend. YI *et al.* [15] studied the influence of interface types on shear characteristics, concluding that they conformed to the Mohr-Coulomb strength theory, with the apparent friction angle of the interface composed of sliding and interlocking friction angles. Through large-scale direct shear tests, WANG *et al.* [16] examined the interface properties of gravel layers reinforced with geogrids, finding a nonlinear relationship between the shear strength of gravel aggregates and interface strength parameters with normal stress. Including geogrids reduced the shear strength of gravel aggregates and the interface. Through direct shear tests, ZHOU *et al.* [17], documented that the interfacial shear stress between HDPE geomembranes and industrial solid waste increased in correlation with the enhancement of shear displacement. The gradient of the stress-displacement curve showed a gradual decline. Upon reaching a certain threshold of shear displacement, the interfacial shear stress stabilized. TIWARI and SATYAM's [18] large-scale direct shear and unconfined compressive strength tests on the interaction at the interface between the subgrade, polypropylene fibers, triaxial geogrids, and biaxial geogrids revealed that the shear strength of the reinforced subgrade increased by 177% with the addition of bi/triaxial geogrids and polypropylene fibers. CEN *et al.* [19] developed a large-scale composite shear test apparatus to study the shear behavior of various geomembrane interfaces, observing higher peak shear stresses and shear displacements on textured geomembrane-soil interfaces compared to smooth ones. ZHANG *et al.* [20] conducted a series of direct shear tests to reveal the shear mechanism of the concrete-HDPE material interface, finding that the interface exhibited evident strain-softening behavior during shearing, with shear strength linearly increasing with normal stress. RAZEGHI and ENSANI [21] compared the shear strength of cohesive sand soil-reinforced interfaces using large direct shear tests, indicating that soils with fine particles could be effectively reinforced using geogrids and geotextiles. However, geogrids were more effective than geotextiles in sandy soils with low fine content. Conversely, geotextiles as reinforcement material outperformed geogrids in soils with a high proportion of fines, especially at high moisture content. The investigative work by MULUTI *et al.* [22], employing a large direct shear apparatus, meticulously compared the shear strength parameters across single and multi-layer geosynthetic interfaces. The study revealed a commendable coherence in the strength envelopes derived from single and multi-layer interface trials. For the range of normal stress, the peak and large displacement strengths from single-interface tests were generally 9% and 24% lower than those from multi-layer interface tests. YANG *et al.* [23] explored the effects of shear materials and shear rates through direct shear tests, finding that the interface friction properties of composite geomembranes and granular materials were enhanced. As the test material's particle size increased, the plastic film surface's friction angle decreased while the fabric interface's friction angle increased. The faster the shear rate, the greater the interface friction angle. FENG *et al.* [24]

utilized the Discrete Element Method (DEM) to generate textured and thermally bonded nonwoven geotextiles with destructible rough surfaces. It was found that the level of fiber bonding significantly impacted the interface shear behavior of textured geomembranes with strong rough surfaces. At the same time, it could be not very important for smooth geomembranes. MOHAMADI MERSE *et al.* [25] found through large-scale direct shear tests that geotextile-encased granular columns significantly improve the shear strength and stiffness of soft clay, with the improvement being influenced by the aggregate's relative density and the applied normal stress. ALMEIDA *et al.* [26] observed that an increase in compaction energy leads to enhanced contact between geosynthetic materials and soil, thereby augmenting the interface friction force. SANJANA *et al.* [27] studied the interaction between geogrids and steel slag as well as construction and demolition waste through direct shear and pull-out tests, finding that their shear strength and pull-out resistance are higher than that of sand, and successfully predicted the pull-out performance of geogrids using an artificial neural network model. ROCHA *et al.* [28], assessed the feasibility of using recycled concrete aggregates (ARCO) in reinforced geogrid walls, finding that ARCO exhibits satisfactory physical and mechanical bonding properties in walls up to 5 meters in height. GUO *et al.* [29] discovered through direct shear tests and analysis using acoustic emission and digital image correlation techniques that the interface damage and shear failure of concrete-polymer composite structures repaired with non-water reactive polymers primarily occur at the interface. PEREIRA *et al.* [30] confirmed that buriti leaf fibers exhibit excellent tensile strength when used as reinforcement in the preparation of unidirectional continuous fiber-reinforced polymer composites, especially when combined with an epoxy resin matrix. SINGH *et al.* [31] proposed a semi-empirical model through experiments, successfully simulating the interface shear behavior of sand and geogrids contaminated with used diesel engine oil, demonstrating a trend of decreasing shear strength as the level of contamination increases. The study by SILVA *et al.* [32], examining the technological properties of cementitious composites crafted from both natural and industrial coconut fibers, demonstrated their capability as eco-friendly replacements for conventional wood particle reinforcement materials. YANG *et al.* [33] found through direct shear tests that the interfacial friction performance of composite geomembranes and cushion materials is influenced by shear material, roughness, shear rate, and test temperature.

The behavior of the interfaces in soil-geosynthetic composites is fundamentally influenced by the parameters extracted from pull-out resistance and shearing interaction tests. A considerable body of research has been devoted in recent times to decipher the intricate mechanisms governing these interface behaviors. Nonetheless, exploring the reinforcing interactions within the matrix of coal gangue and geosynthetics remains notably limited. It is thus critical to delve into the reinforcement processes operative between coal gangue and geosynthetic constituents. This investigation delineates an exhaustive assessment encompassing large-scale direct shear experimental procedures applied to calcined coal gangue interfaced with a trio of geosynthetic variants under a spectrum of normal stress conditions. It examines the role of diverse geosynthetic materials in modulating the interface behaviors when coupled with calcined coal gangue. The empirical evidence provided substantial guidance for strategically selecting geosynthetic materials to enhance the structural integrity of embankments composed of reinforced coal gangue.

2. EXPERIMENTAL MATERIALS AND SCHEME

2.1. Experimental materials

The geosynthetic materials used in the experiments were high-toughness polypropylene woven geotextile (referred to as Geotextile), welded steel-plastic geogrid (Geogrid A), and high-density polyethylene (HDPE) uniaxial geogrid (Geogrid B), as depicted in Figure 1. The width of these materials, designated as B, was set at 1 meter to fit the size of the test box. The technical specifications of Geotextile, Geogrid A, and Geogrid B are detailed in Table 1, Table 2, and Table 3, respectively. The coal gangue used was sourced from the Lubi Building Materials Yard in Laiwu. It had been stored for 40–50 years, amounting to 1.07 million cubic meters. Its physical and mechanical properties were determined through laboratory tests, presented in Table 4 and Table 5. Figure 2 illustrates the grading curve of the coal gangue.

2.2. Experimental scheme

2.2.1. Experimental method

Numerous scholars, both domestically and internationally, such as YANG and SUI [34], XU and SHI [35], and FLEMING *et al.* [36], have conducted significant research on the interface characteristics of reinforced soil using direct shear tests, focusing mainly on the relationship between geosynthetics and fillers. Considering equipment limitations, this study also used the direct shear test method.

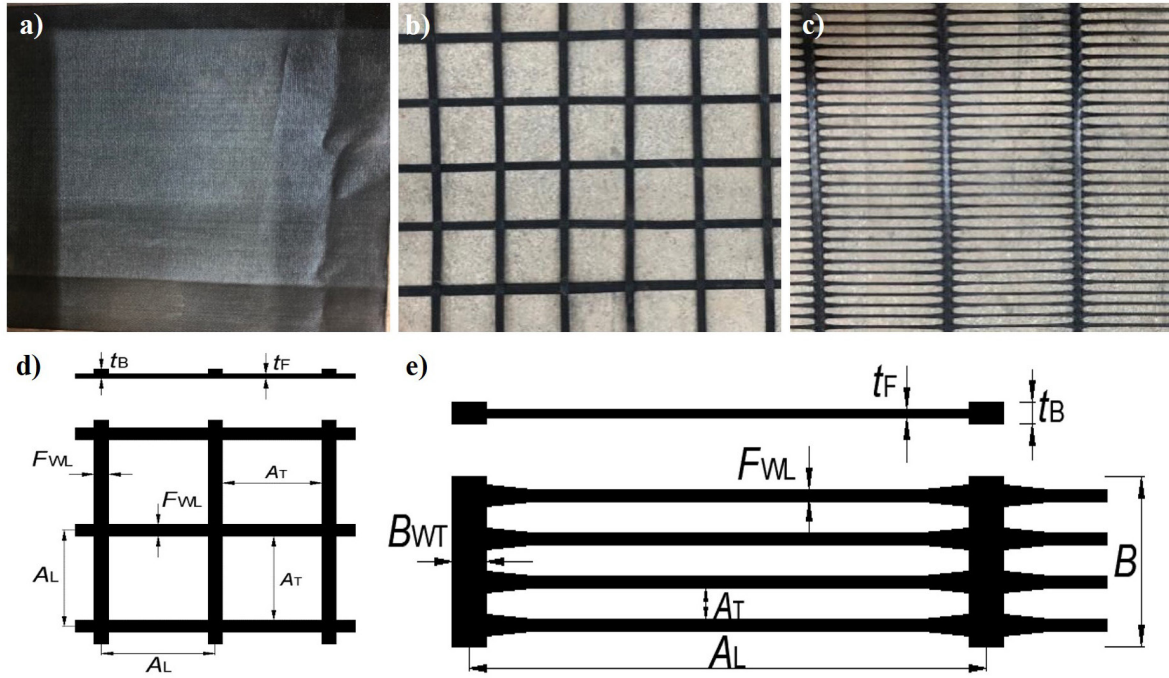


Figure 1: Illustrative representation of diverse geosynthetic materials. (a) Geotextile (b) Geogrid A (c) Geogrid B (d) schematic diagram A (e) schematic diagram B.

Table 1: Technical specifications of geotextile.

MASS PER UNIT AREA (g/m ²)	ULTIMATE TENSILE STRENGTH (kN/m)		ULTIMATE ELONGATION (%)	
	Longitudinal	Transverse	Longitudinal	Transverse
380.00	62.60	103.00	30.25	52.66

Table 2: Technical parameters of Geogrid A.

Ultimate tensile strength (kN/m)	≥80
Rib center spacing A_L (mm)	135.02
2% Strain strength (kN/m)	≥67
Peak strain (%)	≤3
Rib width F_{WL} (mm)	15.74
Net distance of mesh A_T (mm)	119.28
Rib thickness t_F (mm)	2.21
Node thickness t_B (mm)	3.96

The frictional characteristics of the interface between geosynthetic materials and soil are commonly described by apparent friction coefficient (f), internal friction angle (φ), and apparent cohesion (c), following the composite Coulomb's law, satisfying Equation (1).

$$\tau = c + \sigma \cdot \tan \varphi = c + \sigma \cdot f \quad (1)$$

where: τ is the shear strength of the geosynthetic-soil interface (kPa); σ is the normal stress (kPa); c is the apparent cohesion (kPa); f is the apparent friction coefficient; φ is the angle of internal friction (°).

Table 3: Technical parameters of Geogrid B.

Transverse rib center spacing A_L (mm)	263.8
Peak strain (%)	11.6
2% Strain strength (kN/m)	27.2
5% Strain strength (kN/m)	52.8
Ultimate tensile strength (kN/m)	97.3
Longitudinal rib mesh spacing A_T (mm)	16.80
Longitudinal rib width F_{WL} (mm)	5.28
Longitudinal rib thickness t_F (mm)	1.23
Transverse rib width B_{WT} (mm)	18.42
Transverse rib thickness t_B (mm)	3.93

Table 4: Mechanical parameters of coal gangue.

Maximum dry density (g/cm ³)	2.03	UNIFORMITY COEFFICIENT	14.35
Apparent density (g/cm ³)	2.665	CURVATURE COEFFICIENT	1.85
Surface dry density (g/cm ³)	2.372	COHESION (kPa)	32.21
Bulk volume density (g/cm ³)	2.197	INTERNAL FRICTION ANGLE (°)	0.84

Table 5: Grain size distribution of coal gangue.

Particle size (mm)	53~37.5	37.5~31.5	31.5~26.5	26.5~19	19~16
Mass percentage (%)	0	7.5	5.5	10.5	8.5
Particle size (mm)	16~13.2	13.2~9.5	9.5~4.75	4.75~2.36	<2.36
Mass percentage (%)	8.0	13.5	16.5	15.0	15.0

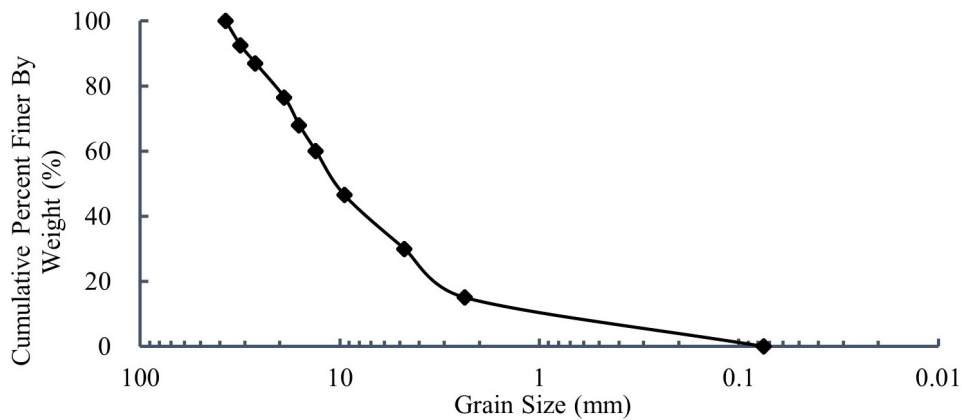


Figure 2: Grain size distribution curve of coal gangue.

Figure 3 illustrates the principle of the direct shear test, in which four different normal stresses are applied to test the shear strength of the interface. Figure 4 shows the shear strength envelope, the slope of which represents the apparent friction coefficient, f , calculated according to Equation (2).

$$f = \frac{\tau}{\sigma} \tag{2}$$

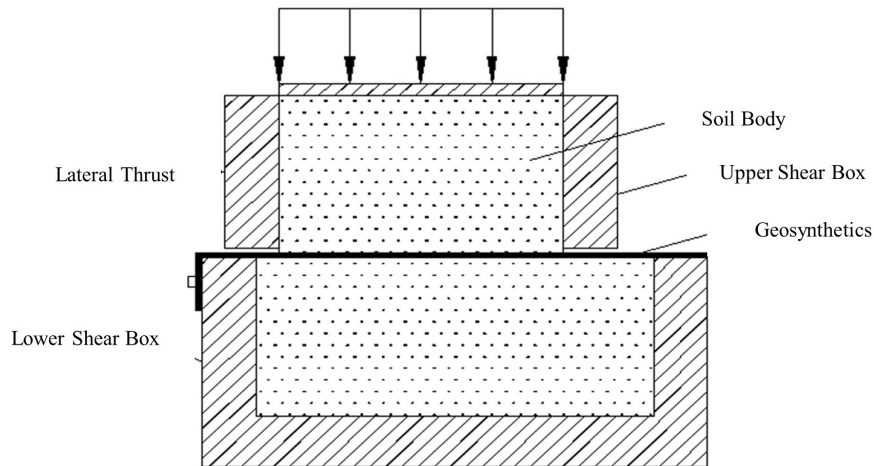


Figure 3: Schematic diagram of the direct shear test principle.

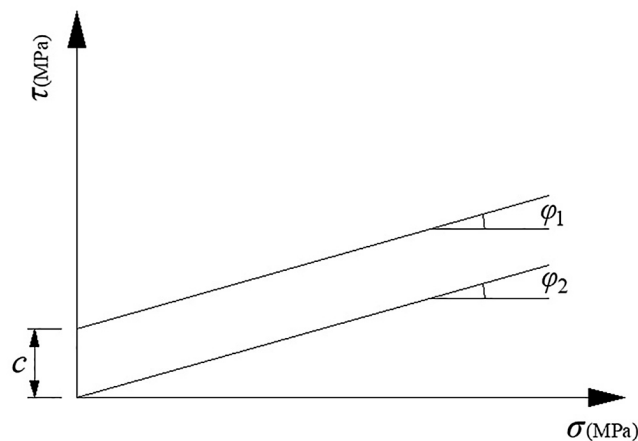


Figure 4: Shear strength envelope for geosynthetic-soil interface.

2.2.2. Experimental apparatus

The experiments employed the pull-out direct shear apparatus provided by Qingdao Xuyu Geomaterial Co., Ltd. This complete experimental setup comprises four main components: a loading system, a traction mechanism, a test box, and a data acquisition system. The internal dimensions of the upper test box are 1000 mm in length, 1000 mm in width, and 370 mm in height, while the lower test box measures 1300 mm in length, 1000 mm in width, and 370 mm in height. The normal stress is generated by a pneumatic counterforce system, capable of reaching up to 400 kPa. The horizontal pulling force is applied through a click system, with a shear rate range from 0 to 5 mm/min. High-precision displacement sensors are installed at both ends of the test box. Shear test data is automatically recorded by high-precision load and displacement sensors, along with supporting software systems.

Figure 5 illustrates the schematic diagram of the apparatus. 1 represents a high-precision displacement meter, 2 denotes the geosynthetic material fixation clamp, 3 identifies the geosynthetic material itself, 4 is the traction motor, 5 and 6 are the fill materials for the lower and upper shear boxes, respectively, 7 is the upper shear box, 8 is the lower shear box, 9 is the rigid pressure plate, 10 is the flexible air pressure bag, and 11 is the reaction cover plate.

2.2.3. Experimental scheme

This study aims to investigate how different geosynthetic materials influence the interface properties of coal gangue-reinforced soil through large-scale direct shear tests. The shear rate for the experiments was set at 1 mm/min.

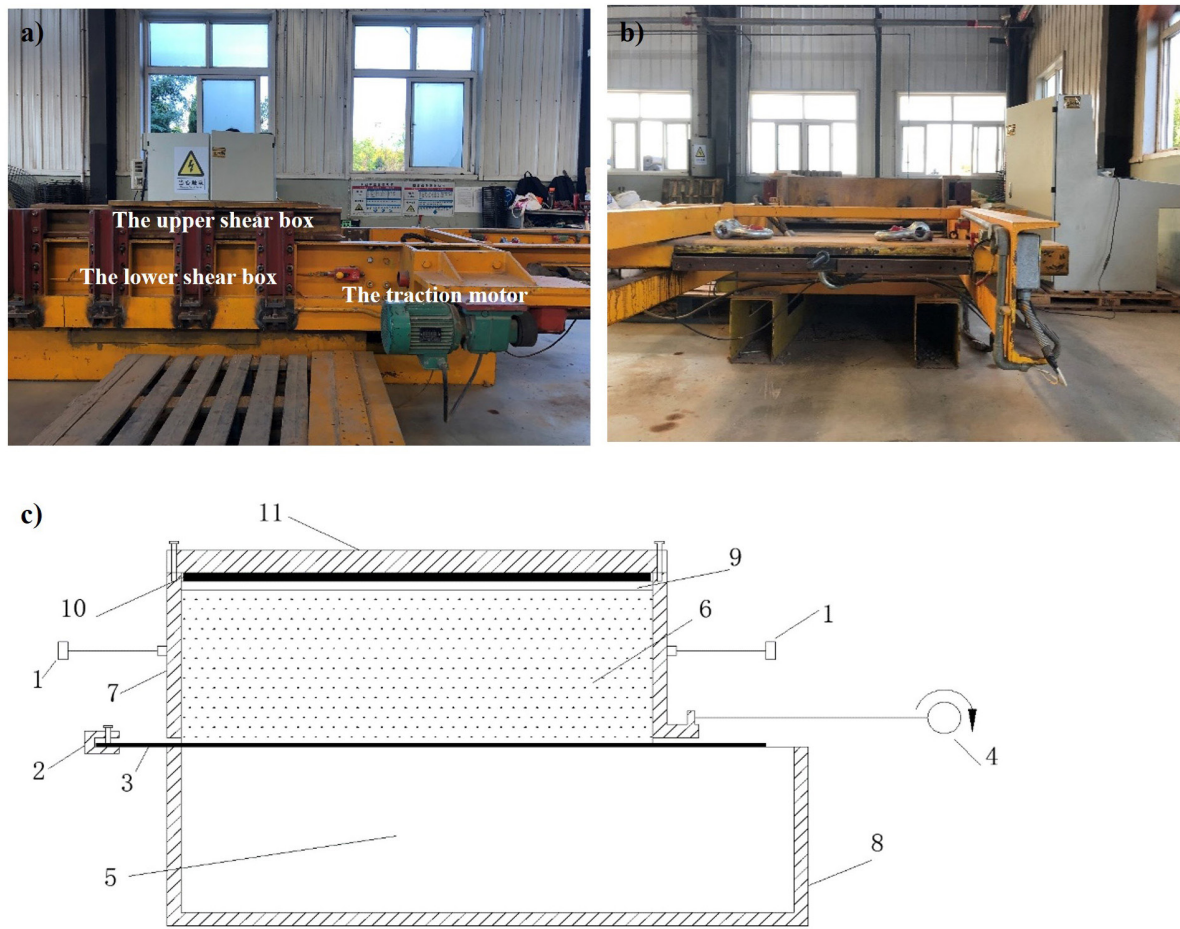


Figure 5: Experimental apparatus. (a) Side view (b) front view (c) schematic diagram.

Table 6: Experimental scheme.

WORKING CONDITION	REINFORCEMENT CONDITION	SHEAR RATE (mm/min)	NORMAL STRESS (kPa)	MAXIMUM SHEAR DISPLACEMENT (mm)
Working condition 1	Unreinforced	1	25	60
Working condition 2	Reinforced with Geotextile	1	50	
Working condition 3	Reinforced with Geogrid A	1	100	
Working condition 4	Reinforced with Geogrid B	1	150	

The geosynthetic material samples were prepared with a width of 1 meter, and the normal stresses applied were 25 kPa, 50 kPa, 100 kPa, and 150 kPa.

Given the substantial size of the test box and to streamline the setup and dismantling process, we incorporated improvements from previous studies [37]. Rigid materials were placed at the bottom, with geosynthetic materials and fillers layered above. Recognizing that the interface between new and old road bases often undergoes settlements due to differences in stiffness, it is a standard engineering practice to install geogrids at these interfaces to mitigate differential settlement. Table 6 refers to the specific experimental scheme.

In the experimental configuration, the fill was set to a height of 25 centimeters, with the compaction of the material sustained at a degree of 93%. Compaction was achieved with an electrical rammer, employed in three distinct stratum, with individual layer heights of 8 cm, 8 cm, and 9 cm, respectively. The delineated procedural steps were as follows:

Activate the apparatus and ascertain the normal functionality of all its components. Introduce the stiff substance into the lower compartment of the shear apparatus. Proceed to trim, position, and affix the geosynthetic fabric. Post the uniform application of petroleum jelly on the inner surfaces of the superior shear compartment, deposit and methodically densify the stipulated volume of coal gangue. Following densification, level off the surface and execute this protocol sequentially for the second and ultimate strata of coal gangue deposition. Conclude by placing a rigid load distributor atop the uppermost layer of coal gangue. Apply a reaction force cover plate and impose a normal load, measured using a precision pressure gauge. The magnitude of the normal load should be maintained stable for ten minutes, ensuring no fluctuations. Once stability is confirmed, the shear rate can be set to initiate the shearing process. After the test, reset the equipment to the initial settings and proceed with the next set of experiments following the previous steps.

3. TEST RESULTS AND ANALYSIS

3.1. Shear stress and shear displacement

Based on the experimental data, shear stress-shear displacement relationship curves were drawn for pure coal gangue and coal gangue reinforced with three geosynthetic materials under four different normal stresses. These are depicted respectively in Figure 6.

Based on the analysis of shear stress and shear displacement relationship curves for coal gangue reinforced with different geosynthetic methods, we draw the following conclusions:

The shear stress-shear displacement relationship curves from the direct shear tests on reinforced and unreinforced coal gangue with geosynthetic materials exhibit nonlinear characteristics. These curves primarily consist of two phases: a rapid increase in shear stress with increasing shear displacement in the first phase,

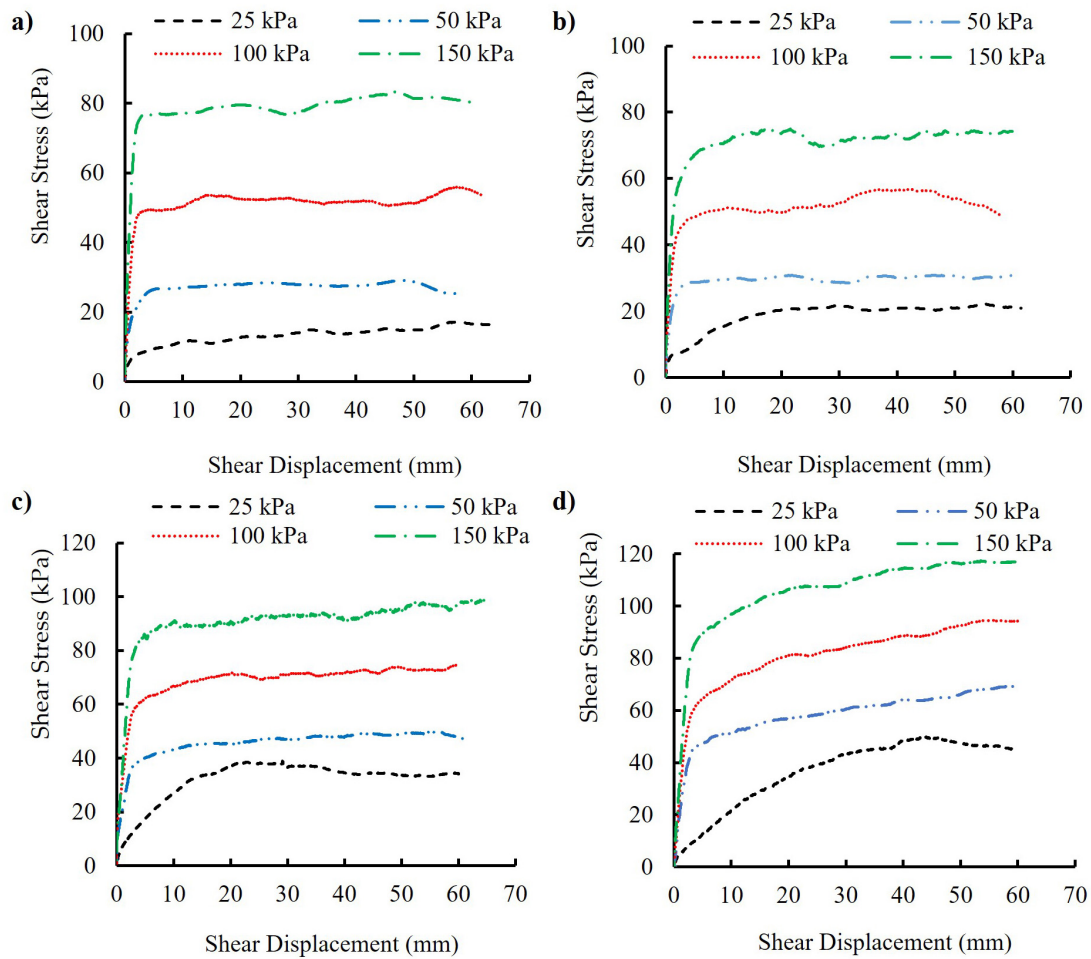


Figure 6: Shear stress-shear displacement relationship curve for coal gangue reinforced with geotextile, Geogrid A, and Geogrid B. (a) Gangue (b) geotextile (c) Geogrid A (d) Geogrid B.

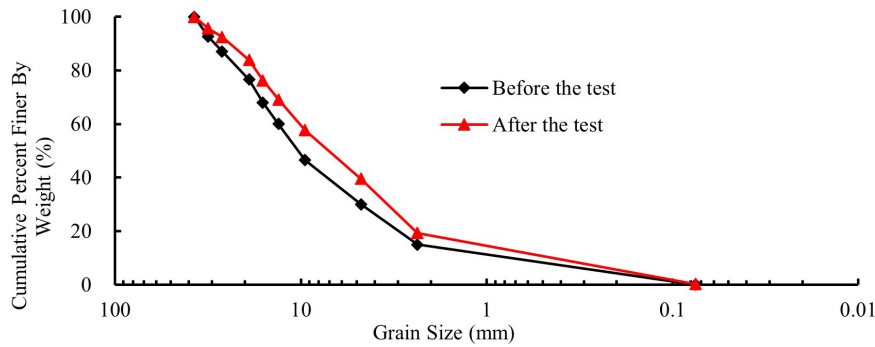


Figure 7: Grain size distribution curves of coal gangue before and after the test.

followed by a gradual stabilization of shear stress, showing a slow increase or decrease in the second phase. It is observed that the use or absence of geosynthetic reinforcement does not significantly alter the overall trend of these curves.

When reinforced with geosynthetic materials, coal gangue’s interface characteristics under low normal stress ($\sigma_v = 25$ kPa) demonstrate a slow linear increase in shear stress with shear displacement, reaching a peak before slightly decreasing. The coal gangue is relatively loose at lower normal stresses, affecting the friction and interlocking with the geosynthetic material. The residual strength results from the shear contraction of coal gangue at the onset of shear deformation under low normal stresses, which then transitions to shear dilation. As the normal stress increases significantly ($\sigma_v = 25$ kPa), the curve swiftly moves into the second phase. This is because, under higher normal stress, the coal gangue particles become denser, leading to a quicker enhancement of the frictional interaction and interlocking bite effect with the surface of the geosynthetic materials.

When using Geogrid B as reinforcement, the relationship between shear stress and displacement demonstrates strain hardening with increasing normal stress. Higher normal stresses lead to greater compaction of coal gangue, enhancing particle interaction and filling in larger particle voids due to particle breakage during shearing (Figure 7 depicts the particle size distribution of coal gangue before and after the experiment). These factors strengthen the interlocking between coal gangue and geogrid, increasing the shear stress.

3.2. Variation of maximum shear stress

Figure 6 shows the evolution trends of maximum shear stress under four different normal stresses, using pure coal gangue and three types of geosynthetic materials as reinforcement. Figure 8 presents the detailed changes in these stresses.

From Figure 8, the following observations can be made:

In the direct shear tests, it was observed that an increase in normal stress leads to a corresponding rise in maximum shear stress. The underlying mechanism of this phenomenon is the gradual compaction of coal gangue particles and the enhancement of their interlocking action due to increased normal stress. Unreinforced coal gangue enhances interface friction with rigid material. However, when reinforced with Geotextile, friction with the Geotextile surface increases, and for Geogrid A and Geogrid B, particles are interlocked within the grid apertures along with enhanced friction.

The variations in maximum shear stress caused by reinforcement with coal gangue are shown in Table 7. The shear stress changes for conditions 2, 3, and 4 are compared to condition 1 in the Table: “-” indicates a decrease, while the absence of “-” means an increase.

From Table 7, the following conclusions can be drawn. When reinforcing coal gangue with three types of geosynthetic materials, the increase in shear stress due to the elevation of normal stress is mitigated. Under the first three levels of normal stress, using Geotextile as the reinforcing material significantly enhances the maximum shear stress of the coal gangue. This indicates that Geotextile effectively strengthens the shear strength of coal gangue within this range of stresses. However, at 150 kPa, the peak shear stress decreases compared to unreinforced coal gangue, as shown in Figure 6b. This phenomenon arises due to increased surface friction between coal gangue particles and Geotextile under higher normal stress. This increased friction leads to localized piercing and damage of the Geotextile surface by the coal gangue particles, causing the edges of the Geotextile to exceed their ultimate tensile strength and rupture, thus reducing the maximum shear stress. Figure 9 shows the condition of the Geotextile’s surface at 150 kPa, where damage or fraying at the edges caused by coal gangue is evident.

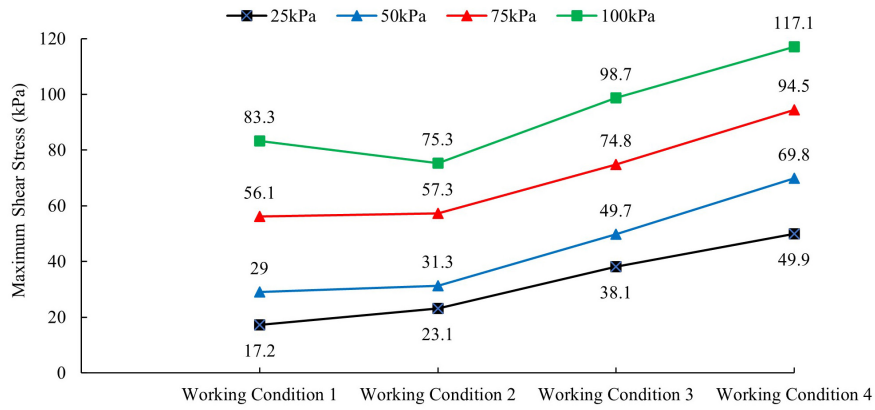


Figure 8: Curves of the maximum shear stress under different reinforcement conditions in coal gangue.

Table 7: Variation of shear stress under different conditions in coal gangue.

NORMAL STRESS (kPa)	WORKING CONDITION						
	SHEAR STRESS (kPa)				SHEAR STRESS GROWTH RATE		
	1	2	3	4	2	3	4
25	17.2	23.1	38.1	49.9	34.2%	121.5%	190.1%
50	29.0	31.3	49.7	69.8	8.1%	71.4%	140.7%
100	56.1	57.3	74.8	94.5	2.0%	33.3%	68.4%
150	83.3	75.3	98.7	117.1	-9.6%	18.5%	40.8%

Note: The last three columns of the table show the growth rate of shear stress for conditions 2, 3, and 4 compared to condition 1.

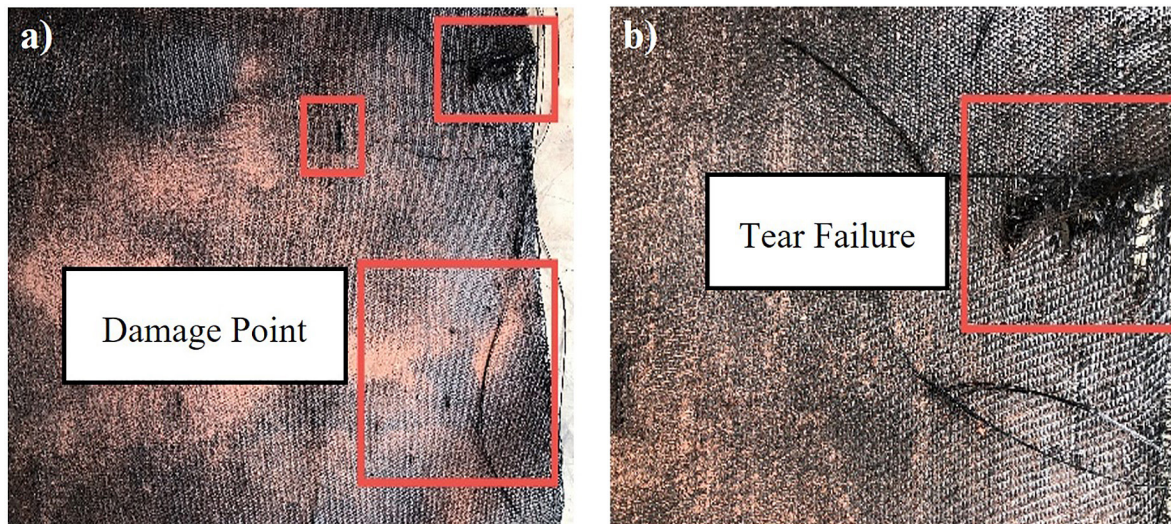


Figure 9: The local surface of geotextile after the test at a normal stress of 150 kPa. (a) Damage point (b) tear failure.

The shear stress of coal gangue reinforced with Geogrid A and Geogrid B exceeds that of Geotextile, especially with the latter, where the increase rate is up to 190.1%. This significant increase is mainly attributed to the characteristics of the geogrids: coal gangue particles not only create friction with the geogrid surface but also interlock tightly with its apertures and transverse ribs. Figure 10 demonstrates the tight interlocking of the geogrid with coal gangue. However, damage at the nodes of Geogrid A results in lower shear stress compared to Geogrid B. Notably, the transverse ribs of Geogrid B are visibly indented. Considering the large external loads

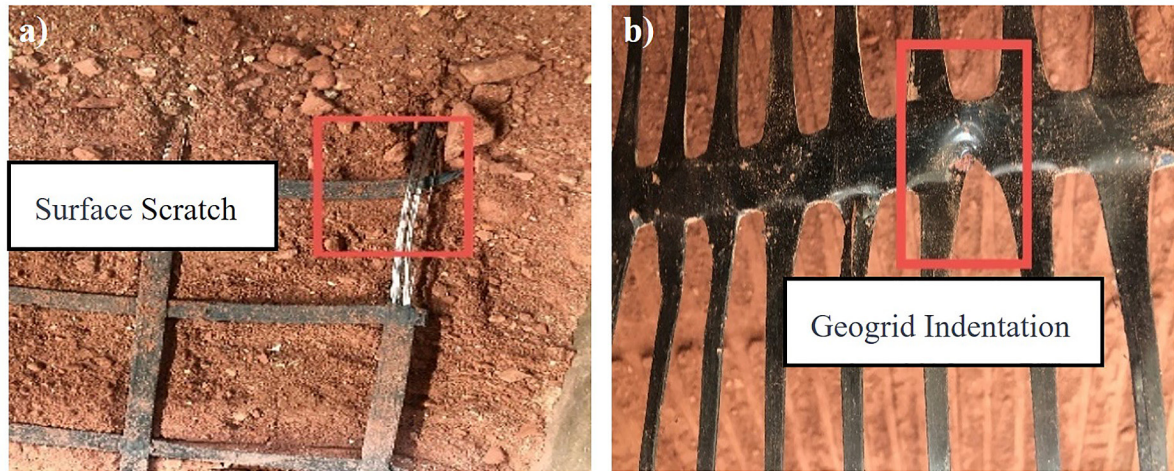


Figure 10: Post-test Geogrid A (left) and Geogrid B (right). (a) Surface scratch (b) geogrid indentation.

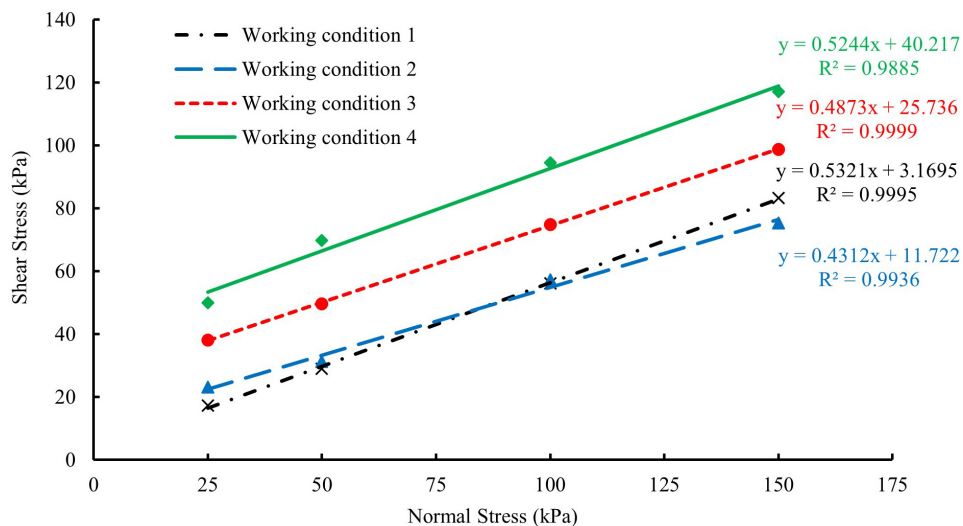


Figure 11: Fitted curves of interface shear strength for coal gangue under different reinforcement conditions.

and sharp particles encountered in engineering applications, Geogrid B is recommended as the reinforcement material in such environments.

3.3. Analysis of interface shear strength indices

The shear strength parameters of the soil-reinforcement interface, including the interface friction angle and apparent cohesion, are derived from fitting the maximum shear stress with the normal stress. Figure 11 displays the shear strength fitting curves for pure coal gangue, Geotextile, Geogrid B, and Geogrid A reinforcement. Figure 11 shows that the correlation coefficients (R^2 values) for the coal gangue direct shear tests under various reinforcement conditions are 0.9995, 0.9936, 0.9999, and 0.9885, respectively, exceeding 0.9500. Since all the values are above 0.9500, it indicates an excellent correlation for the interface shear strength fitting curves. Further, Figure 12 displays the shear strength parameters of the coal gangue interface under different reinforcement conditions.

Table 8 details the variations in shear strength parameters induced by reinforcing with coal gangue. Compared to Condition 1, the shear strength parameters for Conditions 2, 3, and 4 are evaluated; “-” indicates a reduction in the parameter, while the absence of “-” signifies an enhancement.

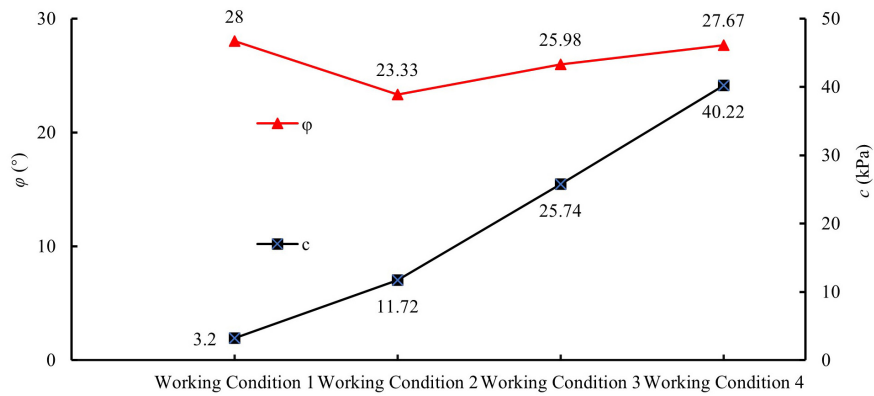


Figure 12: Curves Showing changes in interface shear strength parameters for coal gangue under different reinforcement conditions.

Table 8: Interface shear strength parameters of coal gangue under various reinforcement conditions.

WORKING CONDITION	INTERFACE FRICTION ANGLE ϕ (°)	APPARENT COHESION c (kPa)	VARIATION RANGE	
Working condition 1	28.00	3.20	–	–
Working condition 2	23.33	11.72	–16.7%	266.3%
Working condition 3	25.98	25.74	–7.2%	704.4%
Working condition 4	27.67	40.22	–1.2%	1156.9%

It can be seen from Table 8:

Geosynthetic materials slightly decreased the interface friction angle when comparing reinforced and unreinforced coal gangue. While this reduction varies among different materials, the overall magnitude is small, indicating the minimal impact of various reinforcement materials on the friction angle.

Geosynthetic reinforcement significantly enhances the interface’s apparent cohesion compared to unreinforced coal gangue. Geogrid B shows the most substantial improvement, followed by Geogrid A, with woven Geotextiles exhibiting the least enhancement.

In the reinforcement of coal gangue using three distinct geosynthetic materials, it was observed that the interface friction angle and apparent cohesion were highest with Geogrid B reinforcement, lowest with Geotextile, and Geogrid A exhibited intermediate values. Table 8 corresponds to the maximum shear stress under different reinforcement conditions, showing that Geogrid B performed the best, followed by Geogrid A, and Geotextile demonstrated the least effectiveness. Reinforcement with Geotextile relied primarily on friction between coal gangue particles and the Geotextile surface. In contrast, geogrids contributed to both frictional interaction and an interlocking mechanism with the coal gangue through the apertures and transverse ribs of the grid. Additionally, the incorporation of geogrids induced a shear band of a certain thickness near the shear plane of coal gangue. The particles within the shear band underwent rolling and reorientation, explaining the superior reinforcing effect of geogrids over Geotextiles. Furthermore, due to the relatively denser apertures of Geogrid B compared to those of Geogrid A and the lower nodal strength of Geogrid A, leading to partial nodal failure during shearing, the reinforcing effect of Geogrid A was inferior to that of Geogrid B.

4. CONCLUSIONS

1. The direct shear tests on the geosynthetic materials and coal gangue reveal a nonlinear relationship between shear stress and displacement, primarily divided into two stages. The shear stress increases with the increase in normal stress, and the shearing process involves fracturing coal gangue particles, leading to a noticeable increase in fine particles of coal gangue after the tests.
2. The impact of geosynthetic material types on the interface shear stress of reinforced coal gangue is markedly significant. Utilizing three distinct geosynthetic materials for reinforcement, the observed maximum interface shear stress follows this hierarchy: Geogrid B uniaxial tensile geogrid exhibits the greatest strength,

succeeded by Geogrid A, and the least effective is Geotextile. Particularly at a normal stress of 150 kPa, the interface shear stress of coal gangue reinforced with woven Geotextile demonstrates a reduction in comparison to that of unreinforced coal gangue, suggesting that such woven Geotextiles may not be optimal for coal gangue reinforcement in scenarios involving higher external loads.

3. In this study, particular attention was paid to the impact of three different geosynthetic materials on the interface shear stress of coal gangue. Notably, Geogrid B provided the highest shear stress due to its unique material properties and structure, indicating a distinct advantage in providing soil stability. Conversely, the shear stress performance of the Geotextile was poorer under increased external loads, especially at a normal stress of 150 kPa, indicating its unsuitability for reinforcement projects under higher loads. Compared to pure coal gangue's interface shear strength indices, the reinforcement with geosynthetics did not significantly impact the friction angle but notably increased the apparent cohesion. The order of shear strength indices is consistent with the conclusion (2). Specifically, the apparent cohesion of pure coal gangue is 3.20 kPa, which increases to 11.72 kPa with reinforcement using Geotextile (an increase of 266.3%), 25.74 kPa with Geogrid A (an increase of 704.4%), and 40.22 kPa with Geogrid B (an increase of 1156.9%).
4. After the comprehensive assessment of interface shear stress and shear strength indices, the effectiveness of the three geosynthetic materials in reinforcing coal gangue, in descending order, is Geogrid B performing the best, followed by Geogrid A and Geotextile being the least effective. In practical engineering applications, using Geogrid B as reinforcement material is recommended when facing large external loads or fillers with sharp edges.

5. BIBLIOGRAPHY

- [1] DING, F., "Experimental study on coal gangue filling for subgrade construction", *Highway*, v. 66, n. 2, pp. 69–75, 2021.
- [2] YANG, G., ZHANG, Z., DU, Y., *et al.*, "Study of coal gangue composite reinforced retaining wall embankment slope by using site tests", *Journal of Railway Science and Engineering*, v. 14, n. 7, pp. 1382–1390, 2017.
- [3] WU, J., CHEN, H., WANG, L., *et al.*, "Study on soil interaction characteristics of geosynthetics", *Journal of Geotechnical Engineering*, v. 2001, n. 1, pp. 89–93, 2001.
- [4] HUANG, X., LIU, Z., "Test study on the interface friction characteristics between coal gangue and warp geogrid", *Highway Engineering*, v. 37, n. 5, pp. 123–126, 2012.
- [5] PENG, L., LIU, Z., "Experimental study on the interface friction characteristics of coal gangue and geotextile", *Chinese and Foreign Highways*, v. 33, n. 1, pp. 268–273, 2013.
- [6] YANG, G., GAO, L., DU, Y., "Test study on residual strength characteristics between coal gangue and gabion mesh mixed with different qualities of soil", *Journal of Central South University*, v. 44, n. 12, pp. 5060–5067, 2013.
- [7] XIAO, H., YU, L., LI, L., "Analysis of interface friction characteristics of geosynthetics and sand", *People's Yangtze River*, v. 43, n. 7, pp. 56–58, 2012.
- [8] PENG, L., HUANG, X., LIU, Z., "Test study on the interface friction characteristics between coal gangue and gabion mesh", *Highway Engineering*, v. 37, n. 5, pp. 83–86, 2012.
- [9] ZHOU, F., ZHU, H., DU, Y., "Experimental study on interface properties of constructions and demolition waste and geosynthetics", *Highway Engineering*, v. 45, n. 4, pp. 96–101, 2020.
- [10] WANG, X., ZHANG, J., ZOU, W., *et al.*, "A shear strength model of geogrid-soil interface and its influence factors", *Tumu Gongcheng Xuebao*, v. 46, n. 4, pp. 133–141, 2013.
- [11] MARKOU, N.I., "A study on geotextile-sand interface behavior based on direct shear and triaxial compression tests", *International Journal of Geosynthetics and Ground Engineering*, v. 4, n. 1, pp. 8, 2018. doi: <http://dx.doi.org/10.1007/s40891-017-0121-7>.
- [12] VIEIRA, S.C., PEREIRA, M.P., LOPES, L.D.M., "Recycled construction and demolition wastes as filling material for geosynthetic reinforced structures. Interface properties", *Journal of Cleaner Production*, v. 124, pp. 299–311, 2016. doi: <http://dx.doi.org/10.1016/j.jclepro.2016.02.115>.
- [13] LIU, C., HO, Y.H., HUANG, J., "Large scale direct shear tests of soil/PET-yarn geogrid interfaces", *Geotextiles and Geomembranes*, v. 27, n. 1, pp. 19–30, 2009. doi: <http://dx.doi.org/10.1016/j.geotexmem.2008.03.002>.
- [14] WANG, J., QI, H., HUANG, S., *et al.*, "Large-scale direct shear test on the interface between geogrid and gravel-soil mixture", *Hydrogeology & Engineering Geology*, v. 49, n. 4, pp. 81–90, 2022.

- [15] YI, F., LI, H., ZHANG, J., *et al.*, “Experimental studies on interfacial shear characteristics between polypropylene woven fabrics”, *Materials*, v. 12, n. 22, pp. 3649, 2019. doi: <http://dx.doi.org/10.3390/ma12223649>. PubMed PMID: 31698741.
- [16] WANG, L., ZHU, Q., JIA, Y., *et al.*, “Experimental study on the interface characteristics of reinforced crushed rock cushion layer based on direct shear tests”, *Materials*, v. 16, n. 17, pp. 5858, 2023. doi: <http://dx.doi.org/10.3390/ma16175858>. PubMed PMID: 37687551.
- [17] ZHOU, L., ZHU, Z., YU, Z., *et al.*, “Shear testing of the interfacial friction between an HDPE geomembrane and solid waste”, *Materials*, v. 13, n. 7, pp. 1672, 2020. doi: <http://dx.doi.org/10.3390/ma13071672>. PubMed PMID: 32260223.
- [18] TIWARI, N., SATYAM, N., “An experimental study on strength improvement of expansive subgrades by polypropylene fibers and geogrid reinforcement”, *Scientific Reports*, v. 12, n. 1, pp. 6685, 2022. doi: <http://dx.doi.org/10.1038/s41598-022-10773-0>. PubMed PMID: 35461342.
- [19] CEN, W., WANG, H., SUN, Y., “Laboratory investigation of shear behavior of high-density polyethylene geomembrane interfaces”, *Polymers*, v. 10, n. 7, pp. 734, 2018. doi: <http://dx.doi.org/10.3390/polym10070734>. PubMed PMID: 30960659.
- [20] ZHANG, T., ZHANG, C., ZOU, J., “Interface shear behavior of a shaft lining concrete-high density polyethylene material under different pre-imposed normal stresses”, *PLoS One*, v. 17, n. 3, e0264691, 2022. doi: <http://dx.doi.org/10.1371/journal.pone.0264691>. PubMed PMID: 35298509.
- [21] RAZEGHI, H.R., ENSANI, A., “Clayey sand soil interactions with geogrids and geotextiles using large-scale direct shear tests”, *International Journal of Geosynthetics and Ground Engineering*, v. 9, n. 2, pp. 24, 2023. doi: <http://dx.doi.org/10.1007/s40891-023-00443-0>.
- [22] MULUTI, S.S., KALUMBA, D., SOBHEE-BEETUL, L., *et al.*, “Shear strength of single and multi-layer soil–geosynthetic and geosynthetic-geosynthetic interfaces using large direct shear testing”, *International Journal of Geosynthetics and Ground Engineering*, v. 9, n. 3, pp. 33, 2023. doi: <http://dx.doi.org/10.1007/s40891-023-00450-1>.
- [23] YANG, W., SHI, K., HE, J., “Experimental study on interfacial friction characteristics of composite geomembranes”, *Journal of Asian Architecture and Building Engineering*, v. 21, n. 5, pp. 1959–1967, 2022. doi: <http://dx.doi.org/10.1080/13467581.2021.1964973>.
- [24] FENG, S., WANG, Y., CHEN, H., “DEM simulation of geotextile-geomembrane interface direct shear test considering the interlocking and wearing processes”, *Computers and Geotechnics*, v. 148, pp. 104805, 2022. doi: <http://dx.doi.org/10.1016/j.compgeo.2022.104805>.
- [25] MOHAMADI MERSE, M., HOSSEINPOUR, I., PAYAN, M., *et al.*, “Shear strength behavior of soft clay reinforced with ordinary and geotextile-encased granular columns”, *International Journal of Geosynthetics and Ground Engineering*, v. 9, n. 6, pp. 79, 2023. doi: <http://dx.doi.org/10.1007/s40891-023-00492-5>.
- [26] ALMEIDA, D.C., PITANGA, H.N., SILVA, T.O., *et al.*, “Use of Kruskal-Wallis and Mann-Whitney statistical tests to evaluate geotextile-reinforced soil systems, Brazil”, *Matéria*, v. 27, n. 2, e202145351, 2022. doi: <http://dx.doi.org/10.1590/1517-7076-rmat-2021-45351>.
- [27] SANJANA, S., SURYA, P., AMARNATH, H., “Interaction between biaxial geogrid and solid waste materials: laboratory study and artificial neural network model development”, *International Journal of Geosynthetics and Ground Engineering*, v. 9, n. 6, pp. 77, 2023.
- [28] ROCHA, P., URASHIMA, D.C., GUIMARÃES, M.G.A., “Performance of recycled concrete aggregates in the filling of segmental blocks in segmental retaining walls reinforced with geogrids, Brazil”, *Matéria*, v. 28, n. 1, e20220251, 2022.
- [29] GUO, C., PEI, L., GUAN, H., *et al.*, “Experimental study on interfacial damage mechanisms of polymer-concrete composite structure”, *Journal of Building Engineering*, v. 75, pp. 106968, 2023. doi: <http://dx.doi.org/10.1016/j.jobbe.2023.106968>.
- [30] PEREIRA, W.A., CERON, C., SILVA, M.S., *et al.*, “Development of polymeric composites reinforced with buriti leaf fiber, Brazil”, *Matéria*, v. 26, n. 1, e12932, 2021.
- [31] SINGH, A., PARAMKUSAM, B.R., BASUDHAR, P.K., “Empirical modelling of shear behavior of oil contaminated sand - geogrid interface”, *Soil & Sediment Contamination*, v. 32, n. 1, pp. 31–50, 2023. doi: <http://dx.doi.org/10.1080/15320383.2022.2051426>.
- [32] SILVA, F.M., SCATOLINO, M.V., PAULA, E.A.O., *et al.*, “From coconut waste to the production of cementitious composites as an alternative for civil construction, Brazil”, *Matéria*, v. 28, n. 3, e20220146, 2023.

- [33] YANG, W., SHI, K., HE, J., “Experimental study on interfacial friction characteristics of composite geomembranes”, *Journal of Asian Architecture and Building Engineering*, v. 21, n. 5, pp. 1959–1967, 2022. doi: <http://dx.doi.org/10.1080/13467581.2021.1964973>.
- [34] YANG, G., SUI, C., “Experimental research on interface friction characteristics of geogrids and soil”, *Journal of Shijiazhuang Tiedao University*, v. 23, n. 2, pp. 46–52, 2010.
- [35] XU, C., SHI, Z., “Experimental research on shearing resistance property of sand-geogrid interface under cyclic load”, *Rock and Soil Mechanics*, v. 32, n. 3, pp. 655–660, 2011.
- [36] FLEMING, I.R., SHARMA, J.S., JOGI, M.B., “Shear strength of geomembrane-soil interface under unsaturated conditions”, *Geotextiles and Geomembranes*, v. 24, n. 5, pp. 274–284, 2006. doi: <http://dx.doi.org/10.1016/j.geotexmem.2006.03.009>.
- [37] LEE, K.M., MANJUNATH, V.R., “Soil-geotextile interface friction by direct shear tests”, *Canadian Geotechnical Journal*, v. 37, n. 1, pp. 238–252, 2000. doi: <http://dx.doi.org/10.1139/t99-124>.